

# High-resolution electron microscopy study of a high-copper variant of weldalite 049 and a high-strength Al–Cu–Ag–Mg–Zr alloy

R. A. HERRING\*

604 Aldershot Rd. Baltimore, MD 21229, USA

F. W. GAYLE

National Institute of Standards and Technology, Gaithersburg, MD 20899, USA

J. R. PICKENS

Martin Marietta Laboratories, Baltimore, MD 21227, USA

A high-resolution electron microscopy study was performed on two high-strength aluminium alloys, an Al–6.2Cu–0.4Ag–0.4Mg–0.2Zr alloy and a similar alloy but having a low lithium addition (1.25 wt%), named Weldalite 049, in order to identify their principal strengthening phase. The lattice images of the principal strengthening phase in these alloys were found to be different. The former alloy had the so-called  $\Omega$  phase, which agrees with previous publications, whereas Weldalite 049 had a phase similar to, but not exactly like, the so-called  $T_1$  phase which is the principal strengthening phase of some high lithium ( $\geq 2$  wt%) AlCuLi alloys.

## 1. Introduction

Weldalite 049 is an Al–Cu–Li–Ag–Mg alloy that is strengthened in artificially aged tempers primarily by very thin plate-like precipitates lying on  $\{111\}$  matrix planes [1, 2]. This precipitate might be expected to be the  $T_1$  phase,  $Al_2CuLi$ , which has been observed in Al–Cu–Li alloys. However, in several ways this precipitate is similar to the  $\Omega$  phase which also appears as  $\{111\}$  plates and is found in Al–Cu–Ag–Mg alloys [3–5]. The present study was undertaken to identify the  $\{111\}$  precipitate or precipitates in Weldalite 049 in the T8 (stretched and artificially aged) temper, and to determine whether  $T_1$ ,  $\Omega$ , or some other phase is primarily responsible for the high strength (i.e. 700 MPa tensile strength) in this Al–Cu–Li–Ag–Mg alloy.

## 2. Background metallurgy

Polmear [4] developed a nominal Al–6.3Cu–0.5Ag–0.5Mg–0.5Mn–0.2Zr alloy that had exceptionally high ambient and warm temperature properties for an ingot metallurgy 2xxx (i.e. Al–Cu) alloy. He noted that the Ag + Mg addition stimulated precipitation of the  $\Omega$  phase, whose presence was apparently responsible for the significant strength increase ( $\sim 25\%$ ) over that for conventional high-strength Al–Cu alloys such as 2219 and 2618.

Langan and Pickens [2] performed transmission electron microscopy investigations of Weldalite 049 and a model Al–6Cu–0.4Ag–0.4Mg–0.14Zr alloy

similar to that innovated by Polmear. Langan and Pickens identified the plate-like phase in Weldalite 049 as  $T_1$ , but a cursory investigation of the Al–Cu–Ag–Mg alloy underscored the similarities between  $T_1$  and  $\Omega$ . Moreover, because of the similarity in the diffraction patterns for  $T_1$  and  $\Omega$ , they could not rule out the existence of  $\Omega$  in Weldalite 049 and, consequently, referred to the plate-like precipitates as  $T_1$ -type.

Additions of silver have little or no effect on the strengthening or precipitation behaviour of binary Al–Cu alloys but a marked increase in strength occurs if a small addition of magnesium is also added [3, 4, 6]. The combined presence of Ag and Mg in Al–Cu alloys significantly enhances the formation of the  $\Omega$  phase [3, 6]. The mechanism by which these minor alloying additions jointly stimulate precipitation remains unclear although it is suggested that silver and magnesium may reduce the stacking fault energy in aluminium, which is quite high, resulting in enhanced fault formation of matrix  $\{111\}$  planes which provide nucleation sites for the  $\Omega$  phase [7]. It has also been speculated that silver and magnesium form fine-scale particles on the  $\{111\}$  planes which serve both to nucleate  $\Omega$  and determine its morphology [8], although no evidence was presented to support this theory. More recently, Muddle and Polmear [9] found that silver partitions to the  $\Omega$  phase in an Al–Cu–Ag–Mg alloy and concentrates at the precipitate/matrix interface in the overaged condition, perhaps to help accommodate the misfit strain that is

\* Present address: Tonomura Electron Wavefront Project, ERATO, JRDC, c/o Advanced Research Laboratory, Hitachi Ltd, Hatoyama, Saitama 350-03, Japan

present normal to the habit plane in the matrix. In that study [9], magnesium was not detected and the role of magnesium in  $\Omega$  phase formation is unknown. A recent study by Garg *et al.* [10] has also shown that silver is not required for  $\Omega$  phase formation in Al-Cu-Mg alloys.

### 3. Atomic structure of $\Omega$ and $T_1$ phase

The structure of the  $\Omega$  phase in the Al-Cu-Mg alloy subsystem was proposed by Auld [11, 12] and verified by Knowles and Stobbs [13] to be monoclinic with  $a = b = 0.496$  nm,  $c = 0.848$  nm and  $\gamma = 120^\circ$  (Fig. 1). This structure is equivalent to and more appropriately described as orthorhombic with  $a = 0.496$ ,  $b = 0.859$ , and  $c = 0.848$  nm and space group  $Fmmm$  [9, 13]. Auld showed that this structure is best regarded as a slight distortion of the tetragonal  $\theta$  ( $Al_2Cu$ ) precipitate found in overaged Al-Cu alloys [11, 12].

In the Al-Cu-Li alloy subsystem, controversy exists as to the structure of the  $T_1$  phase – nominally  $Al_2CuLi$ . Hardy and Silcock [14] determined that the  $T_1$  structure belonged to one of the hexagonal space groups  $P622$ ,  $P6mm$ ,  $P6m2$ , or  $P6/mmm$  with  $a = 0.4965$  nm and  $c = 0.9345$  nm, based on a cast, stoichiometric  $Al_2CuLi$  alloy. Vecchio and Williams [15] further determined, using convergent beam electron diffraction, that a cast  $Al_2CuLi$  phase had  $P6/mmm$  symmetry. Huang and Ardell [16] proposed the

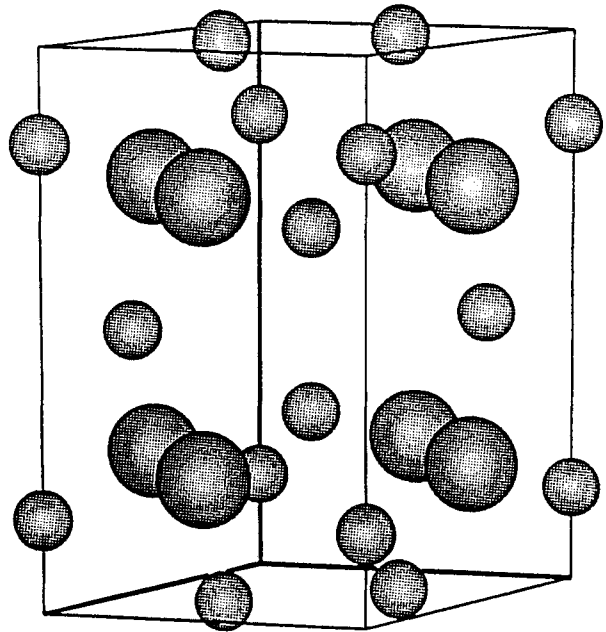


Figure 1 Monoclinic structure of the  $\Omega$  phase showing the corrugated planes in the  $z$  direction where the small balls are aluminium at  $z = 0, 1/6, 1/3, 1/2, 2/3, 5/6,$  and  $1$ , and the large balls are copper at  $z = 1/4$  and  $3/4$ .

space-group symmetry  $P6/mmm$  (Fig. 2a) from calculated X-ray intensities which compared with “fair agreement” with the Debye-Scherrer X-ray intensity measurements reported by Hardy and Silcock [14].

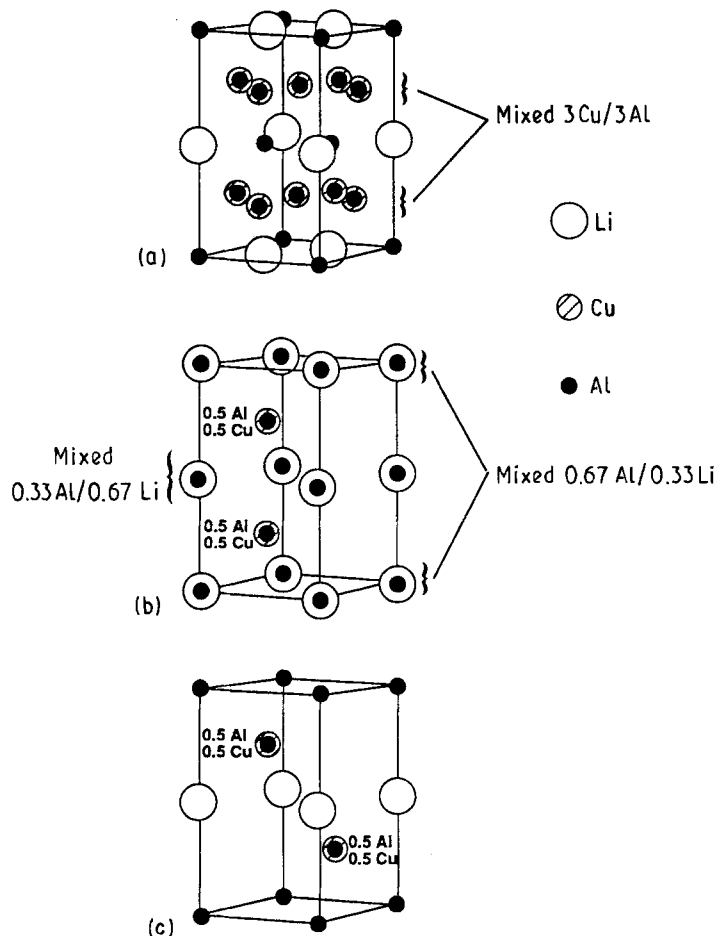


Figure 2 Various models proposed for the  $T_1$  structure: (a) Huang and Ardell [16] having space group  $P6/mmm$ ; (b) Cassada *et al.* [17] sites at  $z = 0$  are occupied by an average of  $0.67$  Al and  $0.33$  Li, whereas at  $z = 1/2$  the occupancy is  $0.33$  Al and  $0.67$  Li; (c) Howe *et al.* [18] having space group  $P\bar{3}m1$ . The structure in (a) has 12 atoms/unit cell and (b) and (c) have 4 atoms/unit cell.

Huang and Ardell [16] suggested the positional stacking of planes to be ABAB . . . , where the A planes are close-packed with ordered arrangements of lithium and aluminium in 2:1 and 1:2 ratios for alternate A planes, and the B planes having a disordered arrangement of copper and aluminium atoms which are not close packed. Cassada *et al.* [17] performed a high-resolution electron microscopy (HREM) study of  $T_1$ . They proposed a modification of Huang and Ardell's structure which consists of four close-packed layers (Fig. 2b).

A model for  $T_1$  was recently proposed by Howe *et al.* [18] based on HREM image calculation. They reported a space group of  $P6mm$ . Their favoured structure consists of four close-packed basal planes within the unit cell, as shown in Fig. 2c, having a stacking sequence of ABAC . . . . Alternate A planes consist of pure aluminium or pure lithium atoms. The B and C planes consist of 50% Al plus 50% Cu which are randomly mixed. Evidence was also given that the B and C planes may vary from the 50/50 Al/Cu mixture.

Thus, several models for  $T_1$  have been proposed and none is completely satisfactory with respect to matching experimental X-ray intensities or HREM images. The various  $T_1$  structures are listed by space group and atomic positions in Table I along with the structure of  $\Omega$  as given by Knowles and Stobbs [13]. In the course of the present work it was found that Howe *et al.*'s structure was not  $P6mm$  (this is most easily seen by a lack of the required two-fold rotation axes for this space group). Indeed, the structure is not hexagonal but is a closely related trigonal space group  $P\bar{3}m1$ . Lattice parameters of the trigonal lattice are  $a = 0.286$  and  $c = 0.935$  nm, giving coherent matching with  $[111]_{Al}$  planes. Though this trigonal structure does not agree with the space groups given by Hardy and Silcock [14], it is possible that the latter, being from a stoichiometric  $Al_2CuLi$  cast structure, is not the same as the  $T_1$  that precipitates within the aluminium matrix.

### 3.1. Experimental procedure

Two alloys were fabricated: a relatively high copper variant of Weldalite 049, and a nominal Al-6Cu-0.4Ag-0.4Mg-0.1Zr alloy. These alloys are the same materials used by Langan and Pickens [2] and will be referred to as Weldalite 049 and Alloy 2, respectively, with measured compositions given in Table II. Each alloy was cast into a 16.5 cm diameter permanent mould and was homogenized by the practices developed by Pickens *et al.* [1]. Each alloy was extruded at a ratio of 21:1 into 10.2 cm bar at a nominal preheat temperature of 370 °C. The Weldalite 049 extrusion was solution treated at 504 °C and Alloy 2 was solution treated at 530 °C, each for 1 h. Each extrusion was water quenched to about 20 °C, stretched 3% and artificially aged at 160 °C for 24 h to the near-peak strength, T8 temper.

TEM specimens were made in the standard way for aluminium alloys [2] and HREM images taken with a Philips EM430T microscope.

## 4. Results

HREM images of the  $\Omega$  phase in Alloy 2 and the  $\{111\}$  strengthening phase (i.e. " $T_1$ -like") in Weldalite 049 were obtained in the  $[112]$  and  $[110]$  matrix orientations. The low symmetry of the  $\Omega$  phase leads to the presence of three variants of  $\Omega$  lying on each  $\{111\}$  matrix plane. Alloy 2 at the  $[110]$  matrix orientation, which is equivalent to the  $[010]$  and  $[310]$  orthorhombic variants of the  $\Omega$  phase, shows  $\{111\}$  precipitates with thin copper-rich (dark) and thick aluminium-rich (light) layers (Fig. 3a) for a multi-unit-cell-thick precipitate. Lattice images of the  $\Omega$  phase show the two variants that exist at the  $[112]$  matrix orientation (equivalent to the  $[100]$  and  $[110]$  orthorhombic orientations of the phase) which produce a square array of dark and light spots in one image (Fig. 3b) and a wavy pattern in another (Fig. 3c).

TABLE I Space groups and atom positions of  $\Omega$  and  $T_1$  structures reported in the literature

Phase	Reference	Structure	Group	Multiplicity/ Wyckoff Letter	Positions			Occupancy
					x	y	z	
$\Omega$	[13]	Orthorhombic $a = 0.496$ nm $b = 0.859$ nm $c = 0.848$ nm	$Fmmm$ (no. 69)	8h	0	1/3	0	8Al
				8i	0	0	1/6	8Al
				8f	1/4	1/4	1/4	8Cu
$T_1$	[18] <sup>a</sup>	Trigonal $a = 0.286$ nm $c = 0.935$ nm	$P\bar{3}m1$ (no. 164)	1a	0	0	0	1Al
				2d	1/3	2/3	1/4	1Al/1Cu
				1b	0	0	1/2	1Li
$T_1$	[17]	Hexagonal $a = 0.286$ nm $c = 0.935$ nm	$P\bar{6}m2$ (no. 187)	1a	0	0	0	0.67Al/0.33Li
				1b	0	0	1/2	0.33Al/0.67Li
				2i	2/3	1/3	1/4	1Al/1Cu
$T_1$	[16]	Hexagonal $a = 0.496$ nm $c = 0.935$ nm	$P6/mmm$ (no. 191)	1a	0	0	0	1Al
				1b	0	0	1/2	1Li
				2c	1/3	2/3	0	2Li
				2d	1/3	2/3	1/2	2Al
				6i	1/2	0	1/4	3Al/3Cu

<sup>a</sup> This is the Howe *et al.* [18] structure rewritten as trigonal.

TABLE II Alloy compositions (wt %)

Alloy	Cu	Li	Ag	Mg	Zr
Weldalite 049	5.83	1.25	0.38	0.42	0.13
Alloy 2	6.16	—	0.41	0.42	0.16

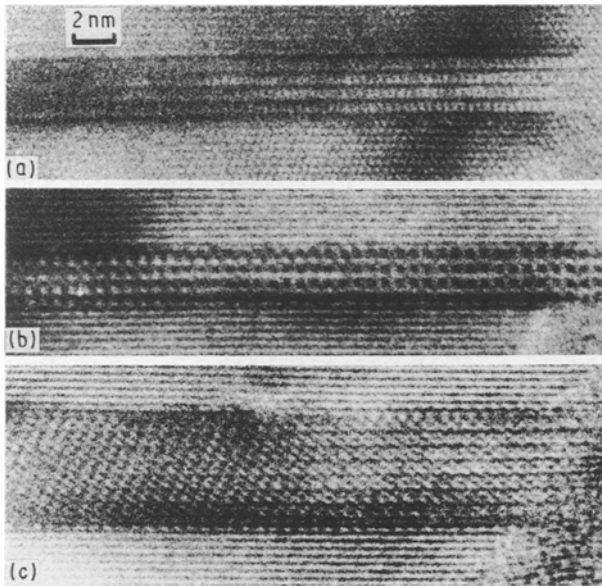


Figure 3 Lattice images of the  $\Omega$  phase in Alloy 2 showing (a) thin copper-rich and thick aluminium-rich layers at the  $[110]$  matrix orientation, (b, c) square array of black and white spots, and wavy light and dark pattern at the  $[112]$  matrix orientation (see text).

For the  $\{111\}$  precipitates in Weldalite 049, the lattice image (Fig. 4) at the  $[110]$  matrix orientation gives an image similar to the  $T_1$  lattice images reported by others in silver and magnesium-free alloys [17, 19]. The  $[112]$  matrix orientation produced only one distinct type of lattice image of the precipitates with examples being given in Fig. 5. These images always have three rows of bright spots per unit cell. Two adjacent rows of spots form a rectangular pattern and the third row of spots, of decreased intensity, are positioned at a (sometimes variable) distance between the rectangular pattern, i.e. they are slightly offset to one side. This pattern of spots is different from previously reported  $T_1$  lattice images at the  $[112]$  matrix orientation which also have three rows of bright spots but which do not form a rectangular array for adjacent rows of spots [17, 19]. The distance between the spots along the precipitate length were measured for both Weldalite 049 and the  $T_1$  images of Cassada *et al.* [16] and Blackburn and Starke [18], using the  $\{111\}$  matrix planes for a reference length in each case, and the white spots in Weldalite 049 were found to have the same separation as those in previously reported  $T_1$  images. The plate-like precipitates in Weldalite 049 thus have a different structure from that of the  $\Omega$  precipitates in Alloy 2. Furthermore, the structure is similar to that of  $T_1$  reported in other Al-Cu-Li alloys, although the pattern viewed along the  $[112]$  matrix orientation is different. Modelling the lattice images by use of the multislice program and atomic configurations given in Table I did not produce any clear match with the experimental images.

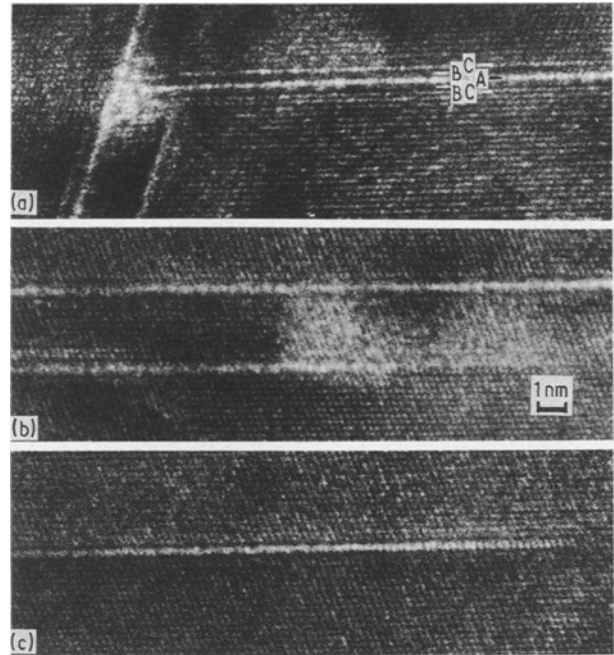


Figure 4 Lattice images of the primary strengthening phase in Weldalite 049 at the  $[110]$  matrix orientation showing the "classic"  $T_1$  structure in (a) where the layers A, B, and C have been designated as being lithium-, copper- and aluminium-rich, respectively (see text).

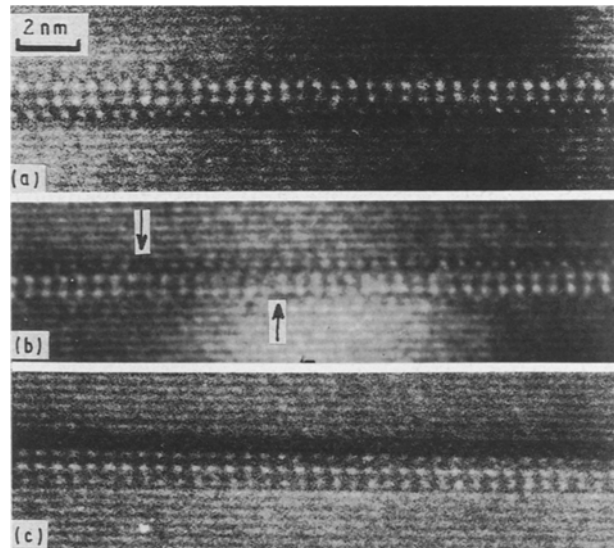


Figure 5 Lattice images of Weldalite 049 showing the "non-classic" structure at the  $[112]$  matrix orientation (see text) where in (b) the arrows point to regions of a missing spot (top) and smeared contrast (bottom), and in (c) the rectangular array of white spots changes from the top two rows to bottom two rows when scanning from left to right.

## 5. Discussion

The lattice images of the  $\Omega$  phase in alloy 2 fit well with those produced by Knowles and Stobbs in an Al-Cu-Ag-Mg alloy [13]. Fig. 3a shows the thick light layers and thin dark layers equivalent to the  $[310]$  orthorhombic orientation image of Knowles and Stobbs. The square array of Fig. 3b is equivalent to the  $[100]_0$  and the wavy array of Fig. 3c is equivalent to the  $[110]_0$  orientation.

The presence of only one type of lattice image at the [1 1 0] and [1 1 2] orientations for alloy Weldalite 049, which is different from that seen in Alloy 2, indicates that the  $\Omega$  phase is not present in Weldalite 049 in the condition investigated. The primary strengthening phase in Weldalite 049 has the previously reported  $T_1$  image at the [1 1 0] matrix orientation. However, at the [1 1 2] matrix orientation, they have a consistently different lattice image from the  $T_1$  images reported by Cassada *et al.* [17] and Blackburn and Starke [19] in the same matrix orientation. It is significant that every {1 1 1} precipitate in Weldalite 049 T8 investigated (dozens) shows this distinct structure. Modelling the lattice images by use of the multislice program and atomic configurations given in Table I did not produce any clear match with the experimental images.

Currently it is difficult to obtain the space group of many thin precipitates. The lattice image is only a two-dimensional image of a three-dimensional structure. Current effort [20] using electron holography, which has been able to obtain an expected point resolution of 0.03 nm [21], involves creating three-dimensional structures with atomic number contrast from two-dimensional images. This capability should enhance our ability to determine the space groups of these thin precipitates.

## 6. Conclusions

High-resolution micrographs of the primary strengthening phase in the T8 temper in each of the two alloys listed in Table I have been obtained. By comparing these experimental images to those images published by Knowles and Stobbs [13] it was found that the  $\Omega$  phase exists in Alloy 2, i.e. the Al-6Cu-0.4Mg-0.4Ag-0.1Zr alloy. By comparing the lattice images of the  $\Omega$  phase to those of Weldalite 049, it was found that the  $\Omega$  phase is not present in the Weldalite 049 alloy under the conditions investigated. In this alloy, the lattice images have the "classic"  $T_1$  lattice image at the [1 1 0] but not at the [1 1 2] matrix orientations. Thus, the primary strengthening phase in Weldalite 049 in the T8 temper examined appears to be  $T_1$  or a closely related variation. This structure may be a faulted (with respect to that seen in silver-free Al-Cu-Li alloys) version of the  $T_1$  phase.

## Acknowledgement

Part of Dr Gayle's time spent in preparing this section was supported by the National Institute of Standards and Technology. The authors are grateful to T. J. Langan for providing the experimental materials in the appropriate tempers and to S. Mannan for his technical assistance.

## References

1. J. R. PICKENS *et al.*, in "Aluminum-Lithium Alloys", Proceedings of the Fifth International Aluminum-Lithium Conference", edited by T. H. Sanders and E. A. Starke (MCE, Birmingham, UK, 1989) p. 1397.
2. T. J. LANGAN and J. R. PICKENS, *ibid.* p. 691.
3. J. T. VIETZ and I. J. POLMEAR, *J. Inst. Metals* **94** (1966) 410.
4. I. J. POLMEAR, in "Aluminum Alloys-Physical and Mechanical Properties", Vol. 1, Conference Proceedings at International Conference, University of Virginia, Charlottesville, VA, 15-20 June 1986 (Chameleon Press) pp. 661-74.
5. R. J. CHESTER and I. J. POLMEAR, *Micron* **10** (1980) 311.
6. I. J. POLMEAR, *Trans. Metall. Soc. AIME* **230** (1964) 1331.
7. S. KERRY and V. D. SCOTT, *Metal Sci.* **18** (1984) 289.
8. J. A. TAYLOR, B. A. PARKER and I. J. POLMEAR, *ibid.* **12** (1978) 478.
9. B. C. MUDDLE and I. J. POLMEAR, *Acta Metall.* **37** (1989) 777.
10. A. GARG, Y. C. CHANGE and J. M. HOWE, *Scripta Metall. Mater.* **24** (1990) p. 677.
11. J. H. AULD, *Acta Crystallogr.* **A28** (1972) S98.
12. *Idem*, *Mater. Sci. Technol.* **2** (1986) 784.
13. K. M. KNOWLES and W. M. STOBBS, *Acta Crystallogr.* **B44** (1988) 207.
14. H. K. HARDY and J. M. SILCOCK, *J. Inst. Metals* **84** (1955-56) 423.
15. K. S. VECCHIO and D. B. WILLIAMS, *Metall. Trans. A* **19** (1988) 2885.
16. J. C. HUANG and A. J. ARDELL, *Mater. Sci. Technol.* **3** (1987) 176.
17. W. A. CASSADA, G. J. SHIFLET and E. A. STARKE Jr, *J. de Phys.* **48** (1988) C397.
18. J. M. HOWE, J. LEE and A. K. VASUDEVAN, *Metall. Trans.* **19A** (1988) p. 2911.
19. L. B. BLACKBURN, E. A. STARKE Jr, in "Aluminum-lithium Alloys", edited by T. H. Sanders Jr and E. A. Starke Jr. Vol. II (MCE, Birmingham, UK, 1989) p. 751.
20. Tonomura Electron Wavefront Project, Exploratory Research for Advance Technology, Research and Development Corporation of Japan.
21. T. KAWASAKI, Q. X. RU, T. MATSUDA and A. TONOMURA, *Jpn J. Appl. Phys.* **30** (1991) 1830.

Received 12 August 1991  
and accepted 7 May 1992.